










DRAFT VERSION AUGUST 7, 2024  
Typeset using L<sup>A</sup>T<sub>E</sub>X **manuscript** style in AASTeX631

## FAST detection of OH emission in the carbon-rich planetary nebula NGC 7027

XU-JIA OUYANG <sup>1</sup>, YONG ZHANG <sup>1,2,3</sup>, CHUAN-PENG ZHANG <sup>4,5</sup>, PENG JIANG,<sup>4,5</sup>  
JUN-ICHI NAKASHIMA <sup>1,3</sup>, XI CHEN <sup>6,7</sup>, HAI-HUA QIAO <sup>8,9</sup>, XU-YING ZHANG,<sup>1</sup> HAO-MIN SUN <sup>1</sup>,  
XIAO-HU LI <sup>2</sup> AND ALBERT ZIJLSTRA <sup>10</sup>

<sup>1</sup>*School of Physics and Astronomy, Sun Yat-sen University, 2 Daxue Road, Tangjia, Zhuhai, Guangdong Province, People's Republic China*

<sup>2</sup>*Xinjiang Astronomical Observatory, Chinese Academy of Sciences, 150 Science 1-Street, Urumqi, Xinjiang 830011, People's Republic of China*

<sup>3</sup>*CSST Science Center for the Guangdong-Hongkong-Macau Greater Bay Area, Sun Yat-Sen University, Guangdong Province, People's Republic China*

<sup>4</sup>*National Astronomical Observatories, Chinese Academy of Sciences, Beijing 100101, People's Republic China*

<sup>5</sup>*Guizhou Radio Astronomical Observatory, Guizhou University, Guiyang 550000, People's Republic China*

<sup>6</sup>*Center for Astrophysics, Guangzhou University, Guangzhou 510006, People's Republic China*

<sup>7</sup>*Shanghai Astronomical Observatory, Chinese Academy of Sciences, 80 Nandan Road, Shanghai 200030, People's Republic China*

<sup>8</sup>*National Time Service Center, Chinese Academy of Sciences, Xi'An, Shaanxi 710600, People's Republic of China*

<sup>9</sup>*Key Laboratory of Time Reference and Applications, Chinese Academy of Sciences, People's Republic China*

<sup>10</sup>*Department of Physics and Astronomy, The University of Manchester, Manchester M13 9PL, UK*

### ABSTRACT

We present the first detection of the ground-state OH emission line at 1612 MHz toward the prototypical carbon-rich planetary nebula (PN) NGC 7027, utilizing the newly installed ultra-wideband (UWB) receiver of the Five-hundred-meter Aperture Spherical radio Telescope (FAST). This emission is likely to originate from the interface of the neutral shell and the

Corresponding author: Yong Zhang  
zhangyong5@mail.sysu.edu.cn

ionized region. The other three ground-state OH lines at 1665, 1667, and 1721 MHz are observed in absorption and have velocities well matched with that of HCO<sup>+</sup> absorption. We infer that the OH absorption is from the outer shell of NGC 7027, although the possibility that they are associated with a foreground cloud cannot be completely ruled out. All the OH lines exhibit a single blue-shifted component with respect to the central star. The formation of OH in carbon-rich environments might be via photodissociation-induced chemical processes. Our observations offer significant constraints for chemical simulations, and they underscore the potent capability of the UWB receiver of FAST to search for nascent PNe.

*Keywords:* Astrophysical masers (103); Hydroxyl masers (771); Planetary nebulae (1249); Circumstellar masers (240)

## 1. INTRODUCTION

Planetary nebulae (PNe), originating from low- and intermediate-mass stars, represent significant objects for material exchange between stars and the interstellar medium. In the asymptotic giant branch (AGB) phase, stars become unstable and expel material into space at a mass-loss rate up to  $10^{-5}$ – $10^{-4} M_{\odot} \text{ yr}^{-1}$  (Vassiliadis & Wood 1993; Bloeker 1995; Decin et al. 2019). Following a brief post-AGB phase ( $10^2$  –  $10^4$  yr; Miller Bertolami 2016), the effective temperature ( $T_{\text{eff}}$ ) of the central star increases rapidly to  $\sim 30$  kK, initiating the ionization of the surrounding circumstellar envelope (CSE) by its radiation, thereby instigating the formation of PN (Kwok 1993). Evolved stars are classified as carbon-rich ( $\text{C/O} > 1$ ), S-type ( $\text{C/O} \approx 1$ ), or oxygen-rich ( $\text{C/O} < 1$ ) based on the carbon to oxygen ratio in their CSEs (Höfner & Olofsson 2018).

Maser emissions of SiO, H<sub>2</sub>O, and OH molecules are frequently detected in the oxygen-rich AGB CSEs (Habing 1996). However, as the AGB evolves into the PN phase, these masers gradually become extinct. It is anticipated that maser emissions, such as SiO, H<sub>2</sub>O, and OH, will sequentially disappear, typically dying out  $\sim 10$ ,  $\sim 100$ , and  $\sim 1000$  years after the end of AGB mass-loss. Consequently, the presence or absence of different maser species can serve as temporal indicators, effectively delineating distinct stages of stellar evolution (Lewis 1989; Gómez et al. 1990). The ground-state OH

transitions originate from four hyperfine sublevels within the lowest rotational state  ${}^2\Pi_{3/2}$ ,  $J = 3/2$ , exhibiting frequencies of 1612.231 ( $F = 1 \rightarrow 2$ ), 1665.402 ( $F = 1 \rightarrow 1$ ), 1667.359 ( $F = 2 \rightarrow 2$ ), and 1720.530 MHz ( $F = 2 \rightarrow 1$ ), respectively. Through the interaction of excitation and de-excitation of rotational excited states ( ${}^2\Pi_{3/2}$ ,  $J = 5/2$  and  ${}^2\Pi_{1/2}$ ,  $J = 1/2$ ), the relative populations of hyperfine sublevels can deviate from their intrinsic values in local thermodynamic equilibrium (LTE) (e.g., Harju et al. 2000; Ebisawa et al. 2015). The OH maser emission at these frequencies exhibit distinct characteristics. Specifically, the 1612 MHz OH maser is predominantly detected within the CSE of evolved stars (e.g., Nguyen-Q-Rieu et al. 1979; Uscanga et al. 2012), whereas the OH masers from the main-line transitions at 1665 and 1667 MHz are mainly associated with massive star-forming regions (Argon et al. 2000; Qiao et al. 2018). The maser at 1721 MHz has primarily been observed in supernova remnants (SNRs; e.g., Frail et al. 1996). While the 1612 MHz OH maser has been commonly detected in evolved stars, it gradually annihilates with the evolution of the central star. As a result, compared to AGB CSEs, PNe rarely exhibit OH masers. Thus far, only eight PNe have been detected or possibly detected in OH maser emission (Zijlstra et al. 1989, 1991; Uscanga et al. 2012; Qiao et al. 2016), which are sometimes called OHPNe or nascent PNe<sup>1</sup>. Except IRAS 07027–7934 (Zijlstra et al. 1991) all these PNe are oxygen-rich. Recently, four additional sources exhibiting OH maser emission were classified as OHPN candidates by matching the interferometric position of OH maser emission with the radio continuum emission position observed in the Southern Parkes Large-Area Survey in Hydroxyl (SPLASH, Cala et al. 2022). Investigating the behavior of OH lines is pivotal for understanding the early evolution of PNe.

In this paper, we report the first detection of ground-state OH lines toward the carbon-rich PN NGC 7027. NGC 7027 is a prototypical young PN and one of the brightest and well-studied object (e.g., Gillett et al. 1967; Becklin et al. 1973; Moseley 1980). Situated at a distance of  $\sim 890$  pc (Ali et al. 2015), it possesses a dynamical age of  $\sim 1000$  years (Zijlstra et al. 2008; Schönberner et al.

<sup>1</sup> The eight OHPNe are V<sub>y</sub> 2–2, IRAS 17393–2727, K 3–35, IRAS 17347–3139, JaSt 23, IRAS 16333–4807, NGC 6302, and IRAS 07027–7934, among which the 1612 MHz OH line detected in NGC 6302 may be dominated by thermal emission (Gómez et al. 2016; Qiao et al. 2020), casting some doubt on its OHPN nature.

2018). Photometric studies reveal a hot central star with an effective temperature of  $\sim 200$  kK (Latter et al. 2000; Zhang et al. 2005; Moraga Baez et al. 2023), exhibiting a ultraviolet (UV) luminosity of  $\sim 3 \times 10^{37}$  erg s $^{-1}$  (Latter et al. 2000; Moraga Baez et al. 2023) and an X-ray luminosity of  $\sim 7 \times 10^{31}$  erg s $^{-1}$  (Kastner et al. 2012; Montez & Kastner 2018). Optical and infrared observations show that NGC 7027 is a carbon-rich nebula (C/O=2.7, Zhang et al. 2005), implying that its progenitor has a mass of  $\sim 2\text{--}4 M_{\odot}$  (Kastner & Wilson 2021, and references therein). The infrared spectroscopy reveals prominent bands from aromatic hydrocarbons, supporting its carbon-rich nature (Beintema et al. 1996; Bernard Salas et al. 2001). Observations of its kinematics revealed an asymmetrical expansion, suggesting the presence of multiple outflows within the nebula (Latter et al. 2000; Cox et al. 2002; López et al. 2012; Lau et al. 2016). The systematic velocity of NGC 7027 is  $\sim 24.3$  km s $^{-1}$  (Bublitz et al. 2023). It was quite unexpected when Liu et al. (1996) discovered the far-infrared rotational lines of H $_2$ O and OH in the Infrared Space Observatory spectrum of this carbon-rich PN. The presence of H $_2$ O was subsequently confirmed by the observation with Herschel Space Observatory (Wesson et al. 2010).

## 2. OBSERVATIONS AND DATA REDUCTION

The observations were carried out on November 18th 2022, employing the newly installed cryogenic ultra-wideband (UWB) receiver of the Five-hundred-meter Aperture Spherical radio Telescope (FAST; Liu et al. 2022; Zhang et al. 2023). The ON-OFF position switching mode was used with a total integration time of 1 hour. The pointing position was set at R.A. = 21<sup>h</sup>07<sup>m</sup>01<sup>s</sup>.57, decl. = +42°14'10".5 (J2000), with the OFF position  $\sim 20'$  away from the ON position. The UWB receiver operates within the frequency range of 500–3300 MHz and is segmented into four subbands, each comprising 1,048,576 channels, providing a frequency resolution of 1049.04 Hz. The velocity resolution achieved for the ground-state OH lines is  $\sim 0.2$  km s $^{-1}$ . We smoothed the spectra to a resolution of  $\sim 1.5$  km s $^{-1}$  to improve the signal-to-noise ratio by averaging over more data points. The half-power beam width (HPBW) is  $\sim 2.5'$  at 1650 MHz. Periodically, a high-intensity noise of  $\sim 12$  K is injected for flux calibration.

After examining the time-frequency diagram, we eliminated the radio frequency interference, and obtained the antenna temperature ( $T_A$ ) through

$$T_A = T_{\text{cal}} \frac{P_{\text{on}}^{\text{cal}}}{P_{\text{on}}^{\text{cal}} - P_{\text{off}}^{\text{cal}}}, \quad (1)$$

where  $T_{\text{cal}}$  is the injected temperature of the noise diode, and  $P_{\text{on}}^{\text{cal}}$  and  $P_{\text{off}}^{\text{cal}}$  denote the power values when the diode is on and off, respectively. The flux density  $S_\nu$  can be deduced through  $S_\nu = T_A/G$ , where  $G$  is the gain (see, [Zhang et al. 2023](#), for details). The linear polarizations XX and YY were calibrated and subtracted with the baseline separately, and then were combined to obtain the final spectra. The detection was deemed genuine only if its flux density exceeded the  $3\sigma$  root-mean-square (rms) noise level, the signal extended across more than multiple adjacent channels, and both linear polarizations XX and YY displayed the signal.

### 3. RESULTS

As shown in [Figure 1](#) and [Figure 2](#), we clearly detect an OH emission line at 1612 MHz and OH absorption lines at 1665, 1667, and 1721 MHz toward the ON position. The behavior of these OH features is strikingly similar to that found in NGC 6302 ([Payne et al. 1988](#)), and is opposite to that in most of Galactic OH sources where the 1612 MHz line is observed in absorption while the 1721 MHz line is in emission ([Hafner et al. 2020](#); [Dawson et al. 2022](#)). These features do not appear in the OFF-position spectrum. The 1612 MHz OH emission in NGC 7027 is fainter than those reported for known OHPNe. All four OH lines show a single component. Gaussian functions were utilized to fit the OH features for the measurements. The fitting results are outlined in [Table 1](#), where the integrated fluxes, the width at half maximum (FWHM), the peak velocities ( $V_P$ ) and fluxes ( $S_P$ ), and the noise root-mean-square (rms) values are given. The central velocities of the main lines and the 1612 MHz emission line suggest an expanding velocity of  $14.9 \text{ km s}^{-1}$  and  $10.6 \text{ km s}^{-1}$ , respectively, indicating that the absorption and emission may come from different regions.

NGC 7027 has been included in the sample of the OH survey performed by [Payne et al. \(1988\)](#) utilizing the NRAO 43-meter telescope, but no firm detection was claimed. As the NRAO 43-meter telescope has a HPBW of  $\sim 18'$  at 1650 MHz, the beam-diluted intensity is about 50 times weaker

than that of the FAST spectrum. Therefore, [Payne et al. \(1988\)](#) were unlikely to see any OH signal in their lower sensitivity spectrum.

It is imperative to validate that the OH emission and absorption indeed originate from this PN rather than from interstellar gas. We scrutinize the databases of masers presented by [Engels & Bunzel \(2015\)](#) and [Ladeyschikov et al. \(2019\)](#), and do not find any record within a radius of  $\sim 17'$  surrounding NGC 7027. Are the OH features associated with a foreground H I cloud? The wide frequency coverage of UWB allows to observe the H I 21 cm line simultaneously. We detect two H I emission lines peaking around  $-20$  and  $10 \text{ km s}^{-1}$  in both ON- and OFF-position spectra, as shown in [Figure 2](#), which are from two extensive clouds. The interferometer observations of [Pottasch et al. \(1982\)](#) show that the two H I lines appear to be absorption against an extragalactic source and the dip at  $-20 \text{ km s}^{-1}$  disappeared when the telescope points toward NGC 7027 (see [Figure 2](#)), suggesting that the positive- and negative-velocity clouds are in front of and beyond NGC 7027, respectively. It is arguable whether the OH absorption is associated with the foreground H I cloud. If so, it is challenging to comprehend that H I is seen in emission while OH is seen in absorption since FAST has similar beam sizes at 18 and 21 cm, though it is not impossible. Given that its velocity is different than the cloud's, the OH emission at 1612 MHz is most likely to originate from the circumstellar shell.

If these OH lines originate from the circumstellar shell, their peak velocities suggest an expansion velocity of  $10\text{--}15 \text{ km s}^{-1}$ , which is consistent with that observed through the nebular CO line profile (see the references in [Hasegawa et al. 2000](#)). The inner ionized gas has a higher expansion velocity, as indicated by the H76 $\alpha$  line ([Figure 1](#); note that it also has a thermal broadening of  $\sim 15 \text{ km s}^{-1}$ ). The interaction between the fast ionized gas and the surrounding neutral materials generates a dense shell, where the photodissociation region (PDR) is situated. [Bublitz et al. \(2023\)](#) discover a slower HCO<sup>+</sup> emission shell and a HCO<sup>+</sup> absorption at  $\sim 10 \text{ km s}^{-1}$ , which are associated with the PN. They infer that HCO<sup>+</sup> originates outside the PDR. [Figure 1](#) shows that the OH emission fits very well with the inner edge of the HCO<sup>+</sup> shell, and thus is likely to be from the PDR. [Figure 2](#) shows the absorption component of HCO<sup>+</sup> that is obtained by summing the negative pixels over a area

$13'' \times 13''$  in the image of [Bublitz et al. \(2023\)](#). It appears that the  $\text{HCO}^+$  and OH absorption come from the same velocity component, probably suggesting that the OH absorption lines originate from the cold layer outside the PDR. The H I absorption spectrum of [Pottasch et al. \(1982\)](#) may display excess absorption at  $\sim 10 \text{ km s}^{-1}$  compared to the extragalactic source, which could be tentatively attributed to a circumstellar component. High angular resolution interferometer observations are needed to validate these findings. In addition, the  $\text{HCO}^+$  spectrum has a shallow dip at  $\sim 3 \text{ km s}^{-1}$ , which should be from the foreground H I cloud.

#### 4. DISCUSSION

OH masers toward AGB stars typically exhibit a double-peaked profile, where the blue- and red-shifted components respectively originate from the approaching and receding sides of the CSE ([Sevenster et al. 1997](#)). In contrast, OH emission in OHPNe displays a pronounced asymmetry, with a notable preference for blue-shifted emission respect to the systemic velocity of the central star ([Zijlstra et al. 1989](#); [Uscanga et al. 2012](#); [Qiao et al. 2016](#)). The blue-shifted OH emission can be attributed to either the obscuration of the red-shifted emission by the ionized gas or the amplification of the continuum emission by the foreground gas. The absence of the red-shifted OH emission accords with the optically thick nature of NGC 7027 at 18 cm. Figure 3 shows the infrared images surrounding NGC 7027 obtained with the Wide-field Infrared Survey Explorer (WISE) space telescope, in which the continuum emission from the NRAO VLA Sky Survey (NVSS, [Condon et al. 1998](#)) is overlaid. NGC 7027 is the strongest infrared and radio emission source within the field, facilitating the production of blue-shifted OH lines.

The 1612 and 1721 MHz OH satellite lines may have a conjugate character with one observed in emission while the other observed in absorption ([Elitzur 1976](#); [Guibert et al. 1978](#)). Such conjugate lines are commonly detected in the sources with bright continuum emission background (eg., [Weisberg et al. 2005](#); [Gómez et al. 2016](#); [Dawson et al. 2022](#)). The decay of the second rotationally excited level can enhance the population of the  $F = 1$  levels on the ground state, resulting in an emission at 1612 MHz and an absorption at 1721 MHz. The pumping is probably done by far-infrared radiation ([Ebisawa et al. 2019](#)). An alternative mechanism is chemical pumping in the hot PDR where OH

is formed and destroyed rapidly, in which the inversion comes from the decay from the high excitation levels after formation (Solomon 1968). Comprehensive theoretical analysis of the excitation of these OH lines in PN circumstances is sorely lacking.

Under an assumption of LTE, the beam-average column density of OH molecules can be estimated from the main absorption lines using the equation given by Liszt & Lucas (1996),

$$N_{\text{OH}} = C_0 \times \Delta T_{\text{ex}} \int \frac{T_A}{\eta} dv \text{ cm}^{-2}, \quad (2)$$

where  $C_0 = 4 \times 10^{14}$  and  $2.24 \times 10^{14} \text{ cm}^{-2} \text{ K}^{-1} \text{ km}^{-1} \text{ s}$  for the 1665 and 1667 MHz transitions respectively (Goss 1968), and the main beam efficiency  $\eta$  is 0.8–0.9 (Sun et al. 2021).  $\Delta T_{\text{ex}}$  is defined by

$$\Delta T_{\text{ex}} = \frac{T_{\text{ex}}}{T_{\text{ex}} - T_{\text{bg}}}, \quad (3)$$

where  $T_{\text{ex}}$  and  $T_{\text{bg}}$  is the excitation temperature of the OH main lines and the background continuum temperature, respectively. For an order of magnitude estimate we assume  $T_{\text{ex}} = 50 \text{ K}$  and  $T_{\text{bg}} = 1000 \text{ K}$ . The resultant  $N_{\text{OH}}$  is about  $10^{14} \text{ cm}^{-2}$ . Given a  $\text{H}_2$  column density of  $N_{\text{H}_2} = (7.7 \pm 3.3) \times 10^{21} \text{ cm}^{-2}$  (Zhang et al. 2008), we obtain a  $N_{\text{OH}}/N_{\text{H}_2}$  abundance ratio of  $\sim 10^{-8}$ , which is comparable to the typical value in diffuse clouds (Wiesemeyer et al. 2012).

NGC 7027 provides only the second case of OH emission in a carbon-rich PN after IRAS 07027–7934 (Zijlstra et al. 1991).<sup>2</sup> The presence of oxygen-bearing molecules in carbon-rich environment has two potential explanations. Oxygen-bearing molecules may be located in a fossil oxygen-rich envelope that has been ejected before the PN progenitor was transformed into a carbon star. If that is the case, OH should be mostly distributed in the outer shell. According to the CO map of NGC 7027 (Bublitz et al. 2023), the molecular shell has a diameter of  $\sim 30''$ . The mass of  $\text{H}_2$  in of NGC 7027 is  $\sim 1 M_{\odot}$  (Santander-García et al. 2012). Assuming a  $\text{OH}/\text{H}_2$  abundance ratio of  $10^{-8}$ , the column density of OH is roughly estimated to be  $\sim 10^{11} \text{ cm}^{-2}$ , about three orders of magnitude lower than the observed value. Therefore, the extended AGB remain envelope is unlikely to produce strong OH absorption as observed here.

<sup>2</sup> The excited-state OH maser at 4765 MHz has been detected in a carbon-rich CSE CRL 618 (Strack et al. 2019), which, however, is usually regarded as a proto-PN.



Instead, the detection of OH infrared lines suggest that this molecule is freshly synthesized in the hot PDR of NGC 7027 through an endothermic reaction  $O + H_2 \rightarrow OH + H$  (Liu et al. 1996), where O is released from CO photodissociation. This scenario is supported by chemical models of NGC 7027 (Yan et al. 1999; Hasegawa et al. 2000). The column density and fractional abundance of OH derived from our observation are in reasonably good agreement with the modelling predictions. OH could also be enhanced through the photodissociation of  $H_2O$ , which is evidently present in NGC 7027 (Wesson et al. 2010). However, the formation of  $H_2O$  in situ in the PDR requires an extremely high temperature ( $\sim 3500$  K), and the formed OH can be rapidly destroyed at these temperatures, either reacting back to  $H_2O$  or dissociating in a reaction with H. Recently, Van de Sande & Millar (2022) show that  $H_2O$  may be present already in the wind of a carbon-rich AGB star if there is UV radiation from a binary companion<sup>3</sup>. This could provide a plausible explanation for the presence of circumstellar OH. Due to its extreme obscuration, it is unclear whether the central star of NGC 7027 has a binary companion. To account for the rings and jets detected in NGC 7027, Moraga Baez et al. (2023) suggest the presence of an unseen binary companion. The detection of circumstellar OH might provide a further evidence for that hypothesis.

## 5. CONCLUSION

Using the UWB receiver of FAST, we detect the 1612 MHz emission line and 1665, 1667, 1721 MHz absorption lines of OH toward the carbon-rich PN NGC 7027. We have compelling evidence supporting the circumstellar origin of the OH emission although we cannot completely rule out the possibility that the the OH absorption lines may be associated with a foreground cloud. These OH ground-state lines exhibit a single blue-shifted component, and behave similarly to those in NGC 6302 albeit with much lower intensities. The detection of OH is uncommon among PNe, and could shed important insights into the transition from the post-AGB to PN phase. Elaborated excitation models are needed to understand the physical conditions of the OH region, for which our observations provide stringent

<sup>3</sup> The AGB envelope contains a substantial amount of dust so that interstellar UV photons cannot penetrate it sufficiently to trigger the photochemistry (see e.g., Willacy & Millar 1997) .

constrains. A search for OH in a larger sample utilizing FAST is expected to substantially increase the number of OHPNe.

## ACKNOWLEDGEMENTS

We acknowledge an anonymous referee for his/her constructive comments. We are very grateful to Jesse Bublitz who helpfully provided us with the the absorption spectrum of  $\text{HCO}^+$ . The financial supports of this work are from the Guangdong Basic and Applied Basic Research Funding (No. 2024A1515010798), the National Natural Science Foundation of China (NSFC, No. 12333005), and the science research grants from the China Manned Space Project (NO. CMS-CSST-2021-A09, CMS-CSST-2021-A10, etc). Y.Z. thank the Xinjiang Tianchi Talent Program (2023). H.-H.Q. is supported by the Youth Innovation Promotion Association CAS and the NSFC(No. 11903038). A.A.Z acknowledges support from STFC/UKRI through grant ST/X001229/1. FAST is operated and managed by the National Astronomical Observatories, Chinese Academy of Sciences.

## REFERENCES

- Ali, A., Ismail, H. A., & Alsolami, Z. 2015, *Ap&SS*, 357, 21, doi: [10.1007/s10509-015-2293-8](https://doi.org/10.1007/s10509-015-2293-8)
- Argon, A. L., Reid, M. J., & Menten, K. M. 2000, *ApJS*, 129, 159, doi: [10.1086/313406](https://doi.org/10.1086/313406)
- Becklin, E. E., Neugebauer, G., & Wynn-Williams, C. G. 1973, *Astrophys. Lett.*, 15, 87
- Beintema, D. A., van den Ancker, M. E., Molster, F. J., et al. 1996, *A&A*, 315, L369
- Bernard Salas, J., Pottasch, S. R., Beintema, D. A., & Wesselius, P. R. 2001, *A&A*, 367, 949, doi: [10.1051/0004-6361:20000435](https://doi.org/10.1051/0004-6361:20000435)
- Bloeker, T. 1995, *A&A*, 299, 755
- Bublitz, J., Kastner, J. H., Hily-Blant, P., et al. 2023, *ApJ*, 942, 14, doi: [10.3847/1538-4357/aca405](https://doi.org/10.3847/1538-4357/aca405)
- Cala, R. A., Gómez, J. F., Miranda, L. F., et al. 2022, *MNRAS*, 516, 2235, doi: [10.1093/mnras/stac2341](https://doi.org/10.1093/mnras/stac2341)
- Condon, J. J., Cotton, W. D., Greisen, E. W., et al. 1998, *AJ*, 115, 1693, doi: [10.1086/300337](https://doi.org/10.1086/300337)
- Cox, P., Huggins, P. J., Maillard, J. P., et al. 2002, *A&A*, 384, 603, doi: [10.1051/0004-6361:20011780](https://doi.org/10.1051/0004-6361:20011780)
- Dawson, J. R., Jones, P. A., Purcell, C., et al. 2022, *MNRAS*, 512, 3345, doi: [10.1093/mnras/stac636](https://doi.org/10.1093/mnras/stac636)
- Decin, L., Homan, W., Danilovich, T., et al. 2019, *Nature Astronomy*, 3, 408, doi: [10.1038/s41550-019-0703-5](https://doi.org/10.1038/s41550-019-0703-5)

- Ebisawa, Y., Inokuma, H., Sakai, N., et al. 2015, *ApJ*, 815, 13, doi: [10.1088/0004-637X/815/1/13](https://doi.org/10.1088/0004-637X/815/1/13)
- Ebisawa, Y., Sakai, N., Menten, K. M., & Yamamoto, S. 2019, *ApJ*, 871, 89, doi: [10.3847/1538-4357/aaf72b](https://doi.org/10.3847/1538-4357/aaf72b)
- Elitzur, M. 1976, *ApJ*, 203, 124, doi: [10.1086/154054](https://doi.org/10.1086/154054)
- Engels, D., & Bunzel, F. 2015, *A&A*, 582, A68, doi: [10.1051/0004-6361/201322589](https://doi.org/10.1051/0004-6361/201322589)
- Frail, D. A., Goss, W. M., Reynoso, E. M., et al. 1996, *AJ*, 111, 1651, doi: [10.1086/117904](https://doi.org/10.1086/117904)
- Gillett, F. C., Low, F. J., & Stein, W. A. 1967, *ApJL*, 149, L97, doi: [10.1086/180066](https://doi.org/10.1086/180066)
- Gómez, J. F., Uscanga, L., Green, J. A., et al. 2016, *MNRAS*, 461, 3259, doi: [10.1093/mnras/stw1536](https://doi.org/10.1093/mnras/stw1536)
- Gómez, Y., Moran, J. M., & Rodríguez, L. F. 1990, *RMxAA*, 20, 55
- Goss, W. M. 1968, *ApJS*, 15, 131, doi: [10.1086/190165](https://doi.org/10.1086/190165)
- Guibert, J., Rieu, N. Q., & Elitzur, M. 1978, *A&A*, 66, 395
- Habing, H. J. 1996, *A&A Rv*, 7, 97, doi: [10.1007/PL00013287](https://doi.org/10.1007/PL00013287)
- Hafner, A., Dawson, J. R., & Wardle, M. 2020, *MNRAS*, 497, 4066, doi: [10.1093/mnras/staa2234](https://doi.org/10.1093/mnras/staa2234)
- Harju, J., Winnberg, A., & Wouterloot, J. G. A. 2000, *A&A*, 353, 1065
- Hasegawa, T., Volk, K., & Kwok, S. 2000, *ApJ*, 532, 994, doi: [10.1086/308610](https://doi.org/10.1086/308610)
- Höfner, S., & Olofsson, H. 2018, *A&A Rv*, 26, 1, doi: [10.1007/s00159-017-0106-5](https://doi.org/10.1007/s00159-017-0106-5)
- Kastner, J. H., & Wilson, E. 2021, *ApJ*, 922, 24, doi: [10.3847/1538-4357/ac1f2e](https://doi.org/10.3847/1538-4357/ac1f2e)
- Kastner, J. H., Montez, R., J., Balick, B., et al. 2012, *AJ*, 144, 58, doi: [10.1088/0004-6256/144/2/58](https://doi.org/10.1088/0004-6256/144/2/58)
- Kwok, S. 1993, *ARA&A*, 31, 63, doi: [10.1146/annurev.aa.31.090193.000431](https://doi.org/10.1146/annurev.aa.31.090193.000431)
- Ladeyschikov, D. A., Bayandina, O. S., & Sobolev, A. M. 2019, *AJ*, 158, 233, doi: [10.3847/1538-3881/ab4b4c](https://doi.org/10.3847/1538-3881/ab4b4c)
- Latter, W. B., Dayal, A., Biegging, J. H., et al. 2000, *ApJ*, 539, 783, doi: [10.1086/309252](https://doi.org/10.1086/309252)
- Lau, R. M., Werner, M., Sahai, R., & Ressler, M. E. 2016, *ApJ*, 833, 115, doi: [10.3847/1538-4357/833/1/115](https://doi.org/10.3847/1538-4357/833/1/115)
- Lewis, B. M. 1989, *ApJ*, 338, 234, doi: [10.1086/167194](https://doi.org/10.1086/167194)
- Liszt, H., & Lucas, R. 1996, *A&A*, 314, 917
- Liu, H.-F., Jiang, P., He, C., et al. 2022, *Research in Astronomy and Astrophysics*, 22, 115016, doi: [10.1088/1674-4527/ac9577](https://doi.org/10.1088/1674-4527/ac9577)
- Liu, X. W., Barlow, M. J., Nguyen-Q-Rieu, et al. 1996, *A&A*, 315, L257
- López, J. A., Richer, M. G., García-Díaz, M. T., et al. 2012, *RMxAA*, 48, 3, doi: [10.48550/arXiv.1110.4698](https://doi.org/10.48550/arXiv.1110.4698)
- Miller Bertolami, M. M. 2016, *A&A*, 588, A25, doi: [10.1051/0004-6361/201526577](https://doi.org/10.1051/0004-6361/201526577)
- Montez, Rodolfo, J., & Kastner, J. H. 2018, *ApJ*, 861, 45, doi: [10.3847/1538-4357/aac5df](https://doi.org/10.3847/1538-4357/aac5df)

- Moraga Baez, P., Kastner, J. H., Balick, B., Montez, R., & Bublitz, J. 2023, *ApJ*, 942, 15, doi: [10.3847/1538-4357/aca401](https://doi.org/10.3847/1538-4357/aca401)
- Moseley, H. 1980, *ApJ*, 238, 892, doi: [10.1086/158052](https://doi.org/10.1086/158052)
- Nguyen-Q-Rieu, Laury-Micoulaut, C., Winnberg, A., & Schultz, G. V. 1979, *A&A*, 75, 351
- Payne, H. E., Phillips, J. A., & Terzian, Y. 1988, *ApJ*, 326, 368, doi: [10.1086/166098](https://doi.org/10.1086/166098)
- Pottasch, S. R., Goss, W. M., Arnal, E. M., & Gathier, R. 1982, *A&A*, 106, 229
- Qiao, H.-H., Walsh, A. J., Gómez, J. F., et al. 2016, *ApJ*, 817, 37, doi: [10.3847/0004-637X/817/1/37](https://doi.org/10.3847/0004-637X/817/1/37)
- Qiao, H.-H., Walsh, A. J., Breen, S. L., et al. 2018, *ApJS*, 239, 15, doi: [10.3847/1538-4365/aae580](https://doi.org/10.3847/1538-4365/aae580)
- Qiao, H.-H., Breen, S. L., Gómez, J. F., et al. 2020, *ApJS*, 247, 5, doi: [10.3847/1538-4365/ab655d](https://doi.org/10.3847/1538-4365/ab655d)
- Roelfsema, P. R., Goss, W. M., Pottasch, S. R., & Zijlstra, A. 1991, *A&A*, 251, 611
- Santander-García, M., Bujarrabal, V., & Alcolea, J. 2012, *A&A*, 545, A114, doi: [10.1051/0004-6361/201219211](https://doi.org/10.1051/0004-6361/201219211)
- Schönberner, D., Balick, B., & Jacob, R. 2018, *A&A*, 609, A126, doi: [10.1051/0004-6361/201731788](https://doi.org/10.1051/0004-6361/201731788)
- Sevenster, M. N., Chapman, J. M., Habing, H. J., Killeen, N. E. B., & Lindqvist, M. 1997, *A&AS*, 122, 79, doi: [10.1051/aas:1997294](https://doi.org/10.1051/aas:1997294)
- Solomon, P. M. 1968, *Nature*, 217, 334, doi: [10.1038/217334a0](https://doi.org/10.1038/217334a0)
- Strack, A., Araya, E. D., Lebrón, M. E., et al. 2019, *ApJ*, 878, 90, doi: [10.3847/1538-4357/ab1f93](https://doi.org/10.3847/1538-4357/ab1f93)
- Sun, X.-H., Meng, M.-N., Gao, X.-Y., et al. 2021, *Research in Astronomy and Astrophysics*, 21, 282, doi: [10.1088/1674-4527/21/11/282](https://doi.org/10.1088/1674-4527/21/11/282)
- Uscanga, L., Gómez, J. F., Suárez, O., & Miranda, L. F. 2012, *A&A*, 547, A40, doi: [10.1051/0004-6361/201219760](https://doi.org/10.1051/0004-6361/201219760)
- Van de Sande, M., & Millar, T. J. 2022, *MNRAS*, 510, 1204, doi: [10.1093/mnras/stab3282](https://doi.org/10.1093/mnras/stab3282)
- Vassiliadis, E., & Wood, P. R. 1993, *ApJ*, 413, 641, doi: [10.1086/173033](https://doi.org/10.1086/173033)
- Weisberg, J. M., Johnston, S., Koribalski, B., & Stanimirović, S. 2005, *Science*, 309, 106, doi: [10.1126/science.1112494](https://doi.org/10.1126/science.1112494)
- Wesson, R., Cernicharo, J., Barlow, M. J., et al. 2010, *A&A*, 518, L144, doi: [10.1051/0004-6361/201014589](https://doi.org/10.1051/0004-6361/201014589)
- Wiesemeyer, H., Güsten, R., Heyminck, S., et al. 2012, *A&A*, 542, L7, doi: [10.1051/0004-6361/201218915](https://doi.org/10.1051/0004-6361/201218915)
- Willacy, K., & Millar, T. J. 1997, *A&A*, 324, 237
- Yan, M., Federman, S. R., Dalgarno, A., & Bjorkman, J. E. 1999, *ApJ*, 515, 640, doi: [10.1086/307047](https://doi.org/10.1086/307047)
- Zhang, C.-P., Jiang, P., Zhu, M., et al. 2023, *Research in Astronomy and Astrophysics*, 23, 075016, doi: [10.1088/1674-4527/acd58e](https://doi.org/10.1088/1674-4527/acd58e)
- Zhang, Y., Kwok, S., & Dinh-V-Trung. 2008, *ApJ*, 678, 328, doi: [10.1086/529428](https://doi.org/10.1086/529428)

Zhang, Y., Liu, X. W., Luo, S. G., Péquignot, D.,  
& Barlow, M. J. 2005, *A&A*, 442, 249,  
doi: [10.1051/0004-6361:20052869](https://doi.org/10.1051/0004-6361:20052869)

Zijlstra, A. A., Gaylard, M. J., te Lintel Hekkert,  
P., et al. 1991, *A&A*, 243, L9

Zijlstra, A. A., te Lintel Hekkert, P., Pottasch,  
S. R., et al. 1989, *A&A*, 217, 157

Zijlstra, A. A., van Hoof, P. A. M., & Perley,  
R. A. 2008, *ApJ*, 681, 1296, doi: [10.1086/588778](https://doi.org/10.1086/588778)

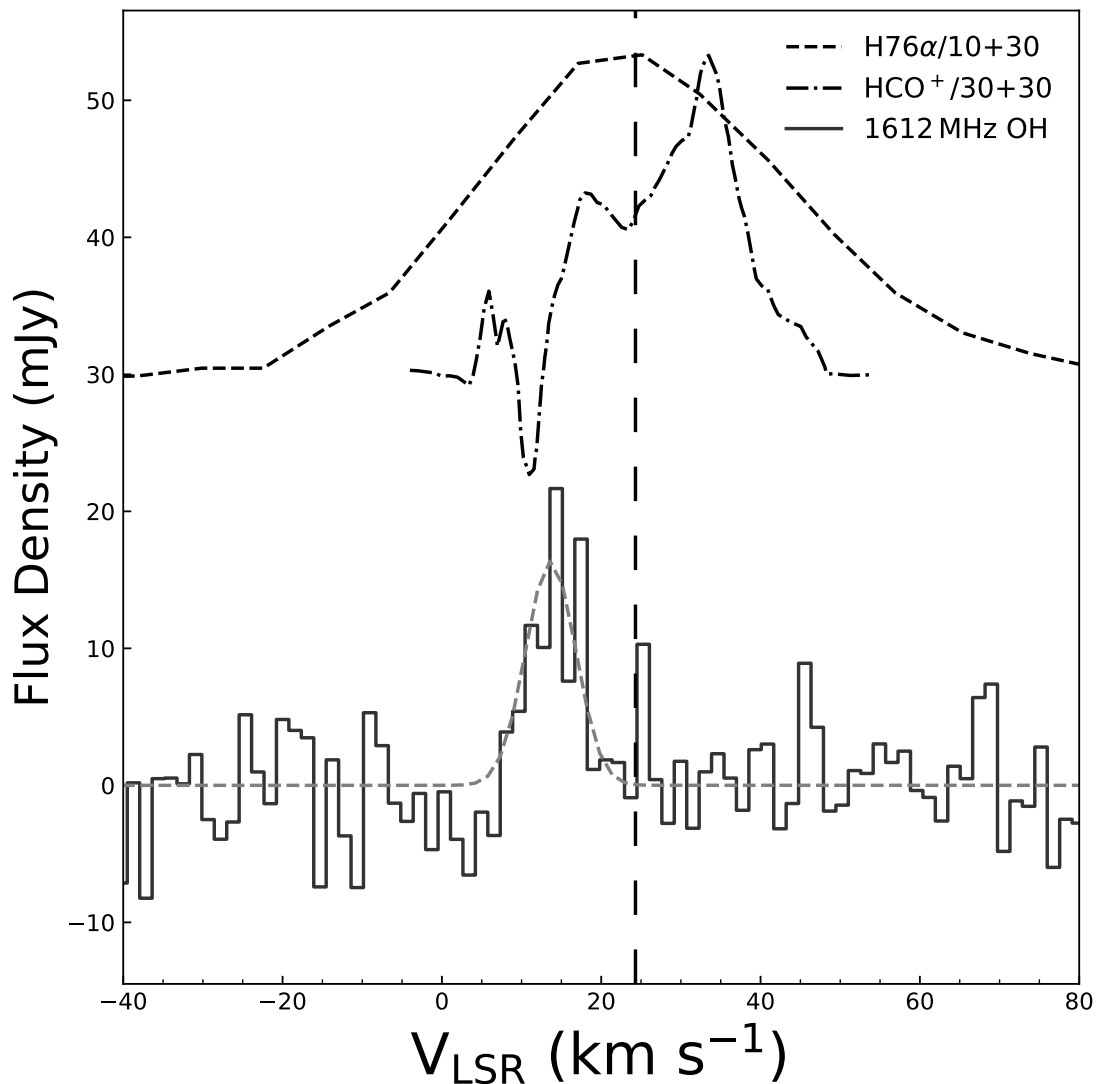


**Figure 1.** The OH emission line at 1612 MHz (solid binned line).  $V_{\text{LSR}}$  is the velocity in the Local Standard of Rest. The gray dashed curve represents the Gaussian fitting result. The vertical straight line indicates the systemic velocity. For comparison, we overplot the profiles of the HCO $^+$  and H76 $\alpha$  lines taken from [Bublitz et al. \(2023\)](#) and [Roelfsema et al. \(1991\)](#), respectively.

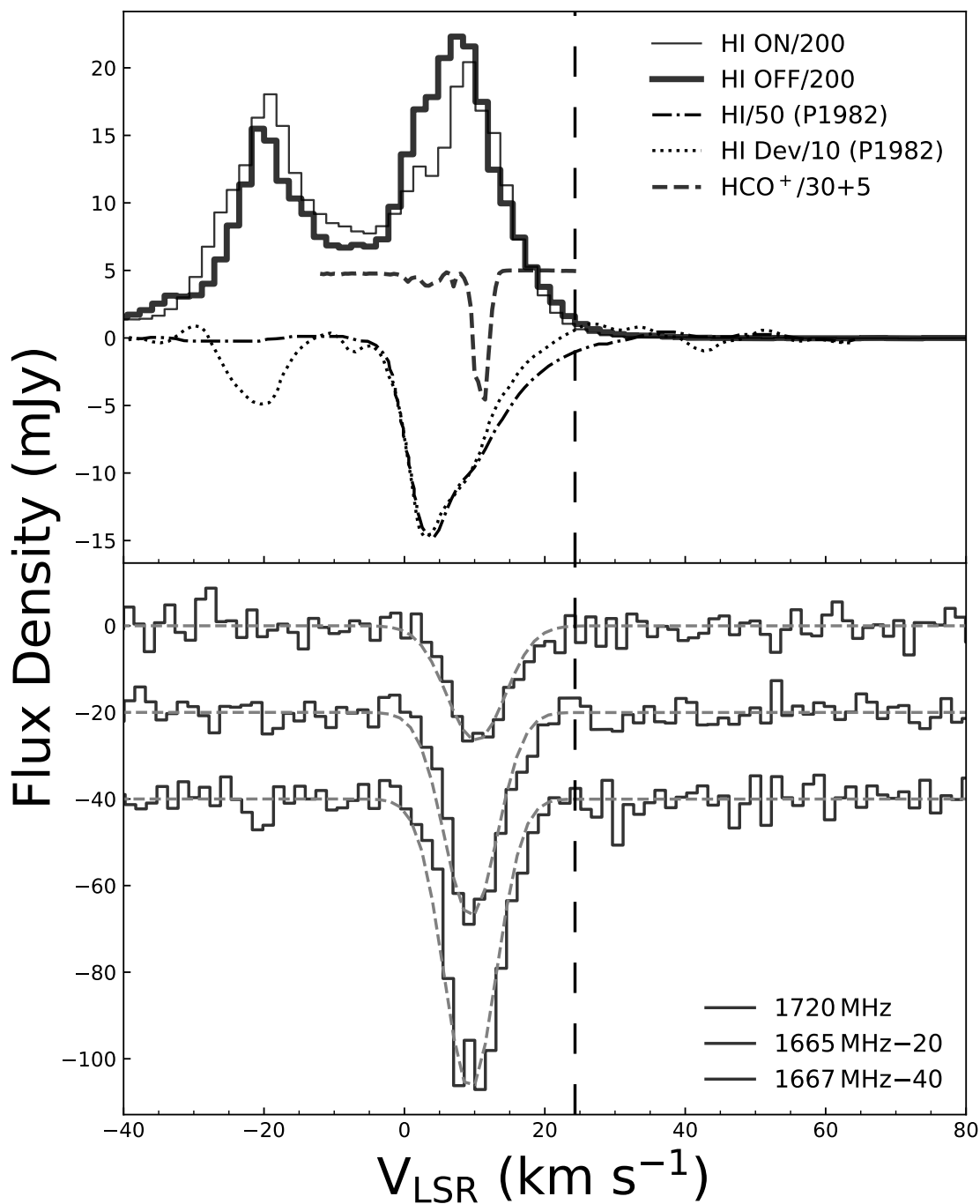


**Figure 2.** Lower panel: Same as Figure 1 but for the OH absorption lines at 1665, 1668, and 1720 MHz. Upper panel: The ON- and OFF-position spectra of H I. For comparison, we overplot the HCO<sup>+</sup> (dashed curves) and H I absorption spectra taken from [Bublitz et al. \(2023\)](#) and [Pottasch et al. \(1982\)](#), where the dot-dashed and dotted curves represent toward NGC 7027 and an extragalactic source, respectively.

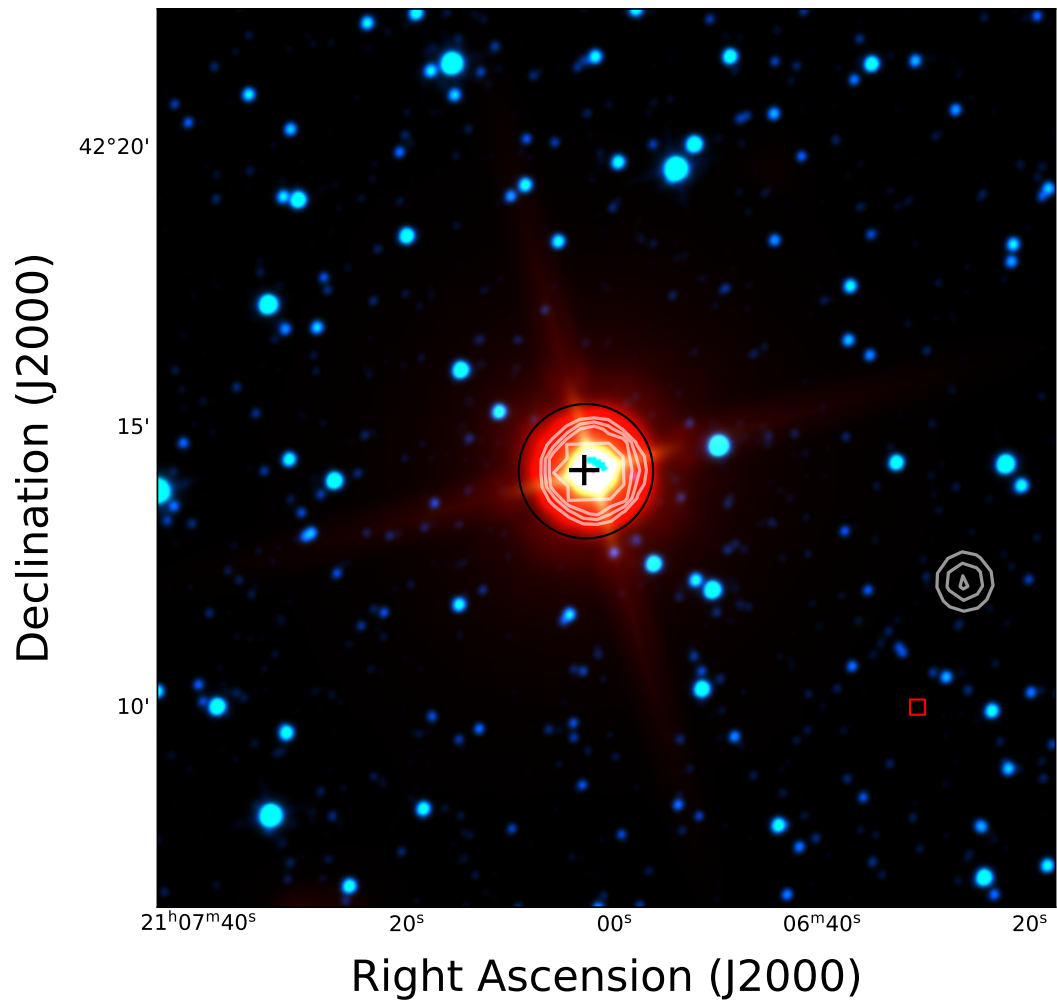


**Figure 3.** The WISE image of NGC 7027. The 3.4, 4.6, and 22  $\mu m$  bands are shown in blue, green, and red, respectively. The black circle and cross indicate the beam size of FAST at 1650 MHz and the beam center. The red square denotes the H II region in this field. The contour of the 1.4 GHz continuum emission is overplotted.



**Table 1.** Measurements of the OH emission and absorption toward NGC 7027.

Frequency (MHz)	$\int S_\nu dv$ (mJy km s <sup>-1</sup> )	$V_p$ (km s <sup>-1</sup> )	FWHM (km s <sup>-1</sup> )	$S_p$ (mJy)	rms (mJy)
(1)	(2)	(3)	(4)	(5)	(6)
1612	128.2±21.8	13.7±0.6	7.4±1.4	16.4±2.8	3.3
1665	-455.6±16.4	9.4±0.2	8.8±0.4	-48.4±1.7	2.7
1667	-638.9±25.0	9.4±0.2	8.7±0.4	-68.7±2.7	3.1
1721	-278.0±15.2	10.2±0.3	9.7±0.6	-26.8±1.5	2.8